

Superconductivity in layered CeO_{0.5}F_{0.5}BiS₂

Rajveer Jha and V.P.S. Awana

Quantum Phenomena and Application Division, National Physical Laboratory (CSIR),
Dr. K. S. Krishnan Road, New Delhi 110012, India

We report appearance of superconductivity in CeO_{0.5}F_{0.5}BiS₂. The bulk polycrystalline samples CeOBiS₂ and CeO_{0.5}F_{0.5}BiS₂ are synthesized by conventional solid state reaction route via vacuum encapsulation technique. Detailed structural analysis showed that the studied CeO_{0.5}F_{0.5}BiS₂ compound is crystallized in tetragonal P4/nmm space group with lattice parameters $a = 4.016(3)$ Å, $c = 13.604(2)$ Å. DC magnetization measurement (MT-curve) shows the ferromagnetic signal at the low temperature region. The superconductivity is established in CeO_{0.5}F_{0.5}BiS₂ at $T_c^{\text{onset}} = 2.5$ K by electrical transport measurement. Under applied magnetic field both T_c onset and $T_c(\rho = 0)$ decrease to lower temperatures and an upper critical field [$H_{c2}(0)$] above 1.2 Tesla is estimated. The results suggest coexistence of ferromagnetism and superconductivity for the CeO_{0.5}F_{0.5}BiS₂ sample.

Key Words: *BiS₂ based new superconductor, structure, ferromagnetic and transport properties.*

PACS number(s): 74.10.+v, 74.70.-b, 74.70. Dd, 75.50.Gg, 74.25.Fy

***Corresponding Author**

Dr. V. P. S. Awana, Principal Scientist

E-mail: awana@mail.nplindia.org

Ph. +91-11-45609357, Fax-+91-11-45609310

Homepage www.teeewebs.com/vpsawana/

Introduction:

The recent discovery of the BiS_2 -based layered superconductors $\text{Bi}_4\text{O}_4\text{S}_3$ [1, 2] and $\text{REO}_{0.5}\text{F}_{0.5}\text{BiS}_2$ (RE -La, Nd, Pr, Yb & Ce) [3-9] had been of tremendous interest for the condensed matter community. These compounds are very similar in crystal structure to the layered high T_c cuprate and Fe-based superconductors. In the high T_c cuprate superconductors, the superconducting CuO_2 layers are separated by blocking layers [10], while in case of Fe-based compounds, the same role is played by the FeAs layers [11]. The new class of superconductors possesses superconducting BiS_2 layers being separated by charge reservoir blocking layers [12, 13]. Both experimental and theoretical studies showed that BiS_2 layered compounds exhibit multiband behaviors with dominant electron charge carriers originating from the Bi 6p_x and 6p_y bands in the normal state [1, 14]. Theoretical studies especially for $\text{LaO}_{0.5}\text{F}_{0.5}\text{BiS}_2$ compound indicated that the Fermi level crosses conduction bands and thus yields electron pockets [15]. There is also a suggestion that BiS_2 based new superconductors could be conventional superconductors with strong electron phonon coupling [16-18]. The structural instability places these compounds in close proximity to the competing ferroelectric and charge density wave (CDW) phases [15]. This is similar to that as the spin-density wave (SDW) instability in iron based superconductors [19]. The experimental studies for BiS_2 -based materials have focused on increasing the charge carrier concentration via chemical substitution within the blocking layer as well as through a reduction of the unit cell volume via the application of an external pressure, for example, recent studies on the BiS_2 -based compounds involving chemical substitution [20, 21]. The LaOBiS_2 and NdOBiS_2 , having analogous BiS_2 layers, had been found to show superconductivity upon electron doping [22]. It has been proposed that superconductivity and ferromagnetism coexist in the $\text{CeO}_{1-x}\text{F}_x\text{BiS}_2$ compounds; the ferromagnetic order state presumably arises due to the local moments of Ce at low temperatures [9]. In this short communication we report superconductivity of $\text{CeO}_{0.5}\text{F}_{0.5}\text{BiS}_2$ with a typical BiS_2 layer. Both compounds CeOBiS_2 and $\text{CeO}_{0.5}\text{F}_{0.5}\text{BiS}_2$ crystallized in the tetragonal $P4/nmm$ space group. We found the $\text{CeO}_{0.5}\text{F}_{0.5}\text{BiS}_2$ compound shows ferromagnetic transition near 4K in magnetization measurements. It is found that the parent phase is a bad metal, and F doped CeOBiS_2 compound exhibits superconductivity at 2.5K along with 4K ferromagnetism.

Experimental:

Bulk polycrystalline samples CeOBiS_2 and $\text{CeO}_{0.5}\text{F}_{0.5}\text{BiS}_2$ were synthesized by standard solid state reaction route via vacuum encapsulation. High purity Ce, Bi, S, CeF_3 , and CeO_2 are weighed in stoichiometric ratio and ground thoroughly in a glove box under high purity argon atmosphere. The mixed powders are subsequently palletized and vacuum-sealed (10^{-3} Torr) in a quartz tube. Sealed quartz ampoule is placed in tube furnace and heat treated at 700°C for 12h with the typical heating rate of $2^\circ\text{C}/\text{min.}$, and subsequently cooled down slowly over a span of six hours to room temperature. This process was repeated twice. X-ray diffraction (XRD) was performed at room temperature in the scattering angular (2θ) range of 10° - 80° in equal 2θ step of 0.02° using *Rigaku Diffractometer* with Cu K_α ($\lambda = 1.54\text{\AA}$). Rietveld analysis was performed using the standard *FullProf* program. The electrical transport and magnetization measurements were performed on Physical Property Measurements System (*PPMS-14T, Quantum Design*) as a function of both temperature and applied magnetic field.

Results and Discussion:

XRD data at room temperature of CeOBiS_2 and $\text{CeO}_{0.5}\text{F}_{0.5}\text{BiS}_2$ samples are shown in Figure 1. Rietveld refinement of XRD patterns is carried out for the both compounds. These compounds are crystallized in tetragonal structure in space group P4/nmm with small impurity peaks of Bi and Bi_2S_3 . Rietveld refined lattice parameters, atomic coordinates, and site occupancy are shown in the Table I. The Rietveld fitted results exhibited that the lattice parameter a axis of CeOBiS_2 is 4.016\AA and the same is increased for $\text{CeO}_{0.5}\text{F}_{0.5}\text{BiS}_2$ sample to 4.037\AA . The c -axis lattice constant is 13.604\AA and 13.407\AA respectively for CeOBiS_2 and $\text{CeO}_{0.5}\text{F}_{0.5}\text{BiS}_2$ samples. The decrease in c -axis parameter indicates that F is doped successfully at the O site as the ionic radius of F is smaller than that of O. These results are in good agreement with the reported phase diagrams for $\text{NdO}_{1-x}\text{F}_x\text{BiS}_2$ and $\text{CeO}_{1-x}\text{F}_x\text{BiS}_2$ compounds [4, 8].

Figure 2 depict temperature dependence of magnetic susceptibility at 10Oe applied field for the superconducting $\text{CeO}_{0.5}\text{F}_{0.5}\text{BiS}_2$ sample, we observed a strong ferromagnetic signal below about 4 K. No diamagnetic signal is observed down to 1.9 K. Perhaps possible lower temperature (below 2.4K, seen in transport measurements, next section) superconducting diamagnetism is prevailed over by ferromagnetism. It seems the Ce sub-lattice is magnetically ordered at below

about 4K. Inset of Fig.2 shows magnetization-hysteresis (MH) curve at 2K, indicating clearly the ferromagnetic nature. Similar magnetization results are obtained for studied CeOBiS₂ as well. This result is in confirmation with an earlier report on CeO_{1-x}F_xBiS₂ compounds [8]. May it be that superconductivity occurs in the BiS₂ layers along with ferromagnetic order in the CeO layer.

Figure 3(a) presents the resistivity versus temperature (ρ -T) plots for the CeO_{0.5}F_{0.5}BiS₂ sample in the applied magnetic field of up to 10 kOe in temperature range of 1.9 – 3K. The result is similar to that as reported for LaO_{0.5}F_{0.5}BiS₂ superconductor. The superconductivity sets at the onset of ρ -T plots and is complete at $\rho = 0$. In this case, with the application of the magnetic field, both the onset and offset T_c shift toward lower temperature. The inset of the same shows the resistivity in expanded temperature range of 1.9–250K of the CeOBiS₂ and CeO_{0.5}F_{0.5}BiS₂. The parent compound is showing semiconducting like behavior from 250K down to 1.9K. The superconducting T_c onset is observed for CeO_{0.5}F_{0.5}BiS₂ compound in resistivity curve at 2.5K and the zero resistivity T_c($\rho = 0$) at 1.9K.

Figure 3 (b) shows the temperature dependence upper critical field $\mu_0 H_{c2}(T)$, which has been fitted through Ginzburg-Landau theory by using $\rho_n = 90\%$ criterion. In the studied temperature range the dependence of field $\mu_0 H_{c2}(T)$ is nearly linear. The upper critical field H_{c2} evolves with temperature from the formula $H_{c2}(T) = H_{c2}(0)(1 - t^2)/(1 + t^2)$ where $t = T/T_c$. From the fitting, we can clearly see that, initially the behavior of H_{c2} with T is linear near T_c and extends up to a temperature of 0.5K and after that the same nearly saturates. The H_{c2}(0) for the sample is found to be about 1.2 Tesla. The H_{c2}(0) value determined by us is in agreement with other reported literature for BiS₂ based superconducting compounds [6,8].

Conclusion:

In conclusion, we have successfully synthesized BiS₂-based CeO_{0.5}F_{0.5}BiS₂ superconductor. MT-curve showed ferromagnetic signal at below 4K. CeOBiS₂ sample showed bad metal behavior and T_c = 2.5K has been observed in CeO_{0.5}F_{0.5}BiS₂ sample. R(T)H of CeO_{0.5}F_{0.5}BiS₂ exhibited an upper critical field of above 1.2Tesla. We have observed coexistence of ferromagnetic and superconductivity for the CeO_{0.5}F_{0.5}BiS₂ compound. Our results are in confirmation with only report of superconductivity in polycrystalline CeO_{0.5}F_{0.5}BiS₂ [8]. Very

recently, after submission of this work, an article has appeared on cond-mat arxiv related to single crystal growth of superconducting $\text{CeO}_{1-x}\text{F}_x\text{BiS}_2$ with magnetic anomalies in low temperature regime [23].

Acknowledgements

The authors are grateful for the encouragement and support from Director NPL for this work. Rajveer Jha would like to thank the CSIR for providing the SRF scholarship to pursue his Ph.D. This work is also financially supported by DAE-SRC outstanding investigator award scheme on search for new superconductors.

Reference:

1. Y. Mizuguchi, H. Fujihisa, Y. Gotoh, K. Suzuki, H. Usui, K. Kuroki, S. Demura, Y. Takano, H. Izawa, O. Miura Phys. Rev. B, **86**, 214518 (2012).
2. S. K. Singh, A. Kumar, B. Gahtori, Shruti; G. Sharma, S. Patnaik, V. P. S. Awana, J. Am. Chem. Soc., **134**, 16504 (2012).
3. Y. Mizuguchi, S. Demura, K. Deguchi, Y. Takano, H. Fujihisa, Y. Gotoh, H. Izawa, O. Miura, J. Phys. Soc. Jpn., **81**, 114725 (2012).
4. S. Demura, Y. Mizuguchi, K. Deguchi, H. Okazaki, H. Hara, T. Watanabe, S. J. Denholme, M. Fujioka, T. Ozaki, H. Fujihisa, Y. Gotoh, O. Miura, T. Yamaguchi, H. Takeya, and Y. Takano, J. Phys. Soc. Jpn., **82** 033708 (2013).
5. R. Jha, A. Kumar, S. K. Singh, V.P.S. Awana, J Supercond Nov Magn **26**, 499 (2013).
6. V.P.S. Awana, A. Kumar, R. Jha, S. K. Singh, A. Pal, Shruti, J. Saha, S. Patnaik, Solid State Communications **157**, 21 (2013).
7. R. Jha, A. Kumar, S. K. Singh, and V. P. S. Awana, J. App. Phy. **113**, 056102 (2013).
8. Jie Xing, Sheng Li, Xiaxin Ding, Huan Yang, and Hai-Hu Wen, Phys. Rev. B **86**, 214518 (2012).
9. D. Yazici, K. Huang, B.D. White, A.H. Chang, A.J. Friedman and M.B. Maple, Philosophical Magazine **93**, 673 (2013).
10. J. G. Bednorz and K.A. Muller, Z. Phys. B **64**, 189 (1986).
11. Y. Kamihara, T. Watanabe, M. Hirano, H. Hosono, J. Am. Chem. Soc. **130**, 3296 (2008).

12. H. Kotegawa, Y. Tomita, H. Tou, H. Izawa, Y. Mizuguchi, O. Miura, S. Demura, K. Deguchi, and Y. Takano, J. Phys. Soc. Jpn., **81** 103702 (2012).
13. B. Li, Z. W. Xing and G. Q. Huang, Euro Phys. Lett., **10**, 47002 (2013).
14. H. Usui, K. Suzuki, and K. Kuroki, Phys. Rev. B **86**, 220501(R) (2012).
15. X. Wan, H. C. Ding, S. Y. Savrasov, and C. G. Duan, Phys. Rev. B **87**, 115124 (2013).
16. G. B. Martins, A. Moreo, and E. Dagotto, Phys. Rev. B **87**, 081102(R) (2013).
17. I. R. Shein, A. L. Ivanovskii, *Teoret. Fiz.* **96**, 859 (2012).
18. T. Yildirim, Phys. Rev. B **87**, 020506(R) (2013).
19. K. Deguchi, Y. Mizuguchi, S. Demura, H. Hara, T. Watanabe, S. J. Denholme, M. Fujioka, H. Okazaki, T. Ozaki, H. Takeya, T. Yamaguchi, O. Miura and Y. Takano, Euro. Phys. Lett., **101** 17004 (2013).
20. S.G. Tan, L. J. Li, Y. Liu, P. Tong, B.C. Zhao, W.J. Lu, Y.P. Sun, Physica C **483**, 94 (2012).
21. Corentin Morice, Emilio Artacho, y Sian E. Dutton, Daniel Molnar, Hyeong-Jin Kim, and Siddharth S. Saxena, arXiv:1305.1201v1 (2013).
22. Y. Mizuguchi, H. Fujihisa, Y. Gotoh, K. Suzuki, H. Usui, K. Kuroki, S. Demura, Y. Takano, H. Izawa, and O. Miura, Phys. Rev. B **86**, 220510(R) (2012).
23. M. Nagao, A. Miura, S. Demura, K. Deguchi, S. Watauchi, T. Takei, Y. Takano, N. Kumada and I. Tanaka, arXiv:1310.1213.

Table 1 Atomic coordinates, Wyckoff positions, and site occupancy for studied $\text{CeO}_{0.5}\text{F}_{0.5}\text{BiS}_2$.

Atom	x	y	z	site	Occupancy
Ce	0.2500	0.2500	0.099(3)	$2c$	1
Bi	0.2500	0.2500	0.625(5)	$2c$	1
S1	0.2500	0.2500	0.378(1)	$2c$	1
S2	0.2500	0.2500	0.811(2)	$2c$	1
O/F	0.7500	0.2500	0.000	$2a$	0.5/0.5

Figure Captions:

Figure 1 (a): Observed (*Red circles*) and calculated (*solid lines*) XRD pattern of CeOBiS_2 and $\text{CeO}_{0.5}\text{F}_{0.5}\text{BiS}_2$ compounds at room temperature.

Figure 2: Temperature dependence of the dc magnetization of the $\text{CeO}_{0.5}\text{F}_{0.5}\text{BiS}_2$ compound. Inset of the figure shows Isothermal MH curve at 2 K of the sample $\text{CeO}_{0.5}\text{F}_{0.5}\text{BiS}_2$.

Figure 3: (a) Resistivity vs. temperature ($\rho - T$) behavior of $\text{CeO}_{0.5}\text{F}_{0.5}\text{BiS}_2$ with and without applied fields. Inset of the figure shows the $\rho - T$ for CeOBiS_2 and $\text{CeO}_{0.5}\text{F}_{0.5}\text{BiS}_2$ in the temperature range 250 K to 1.9 K. (b) Temperature dependent upper critical field (H_{c2}) fitted by the GL equation for the $\rho_n = 90\%$ of $\text{CeO}_{0.5}\text{F}_{0.5}\text{BiS}_2$ sample.

Figure 1

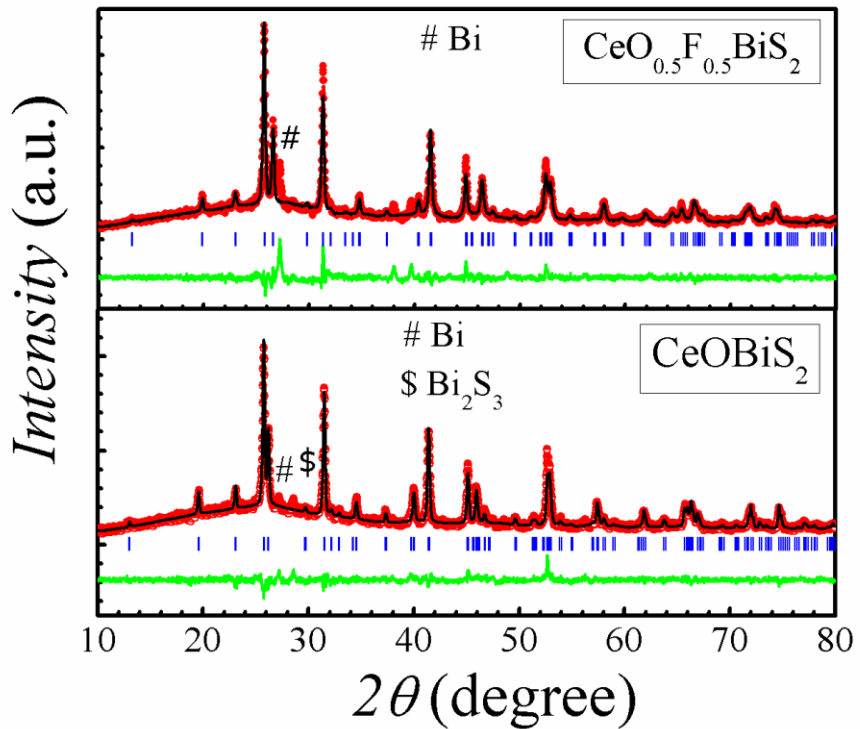


Figure 2

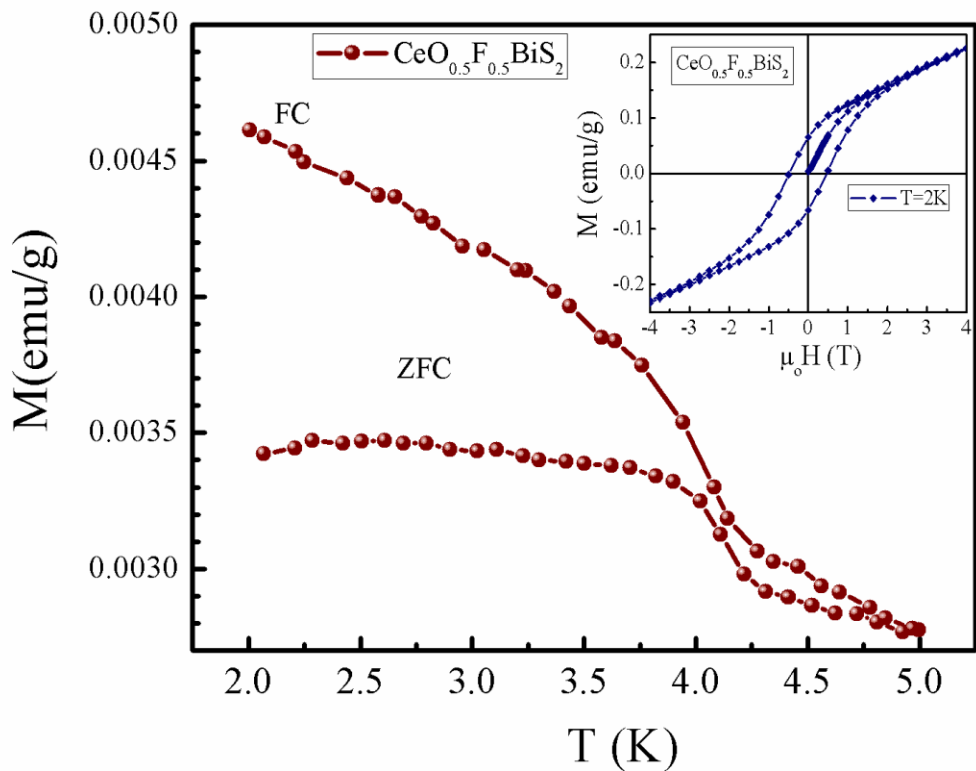


Figure 3(a):

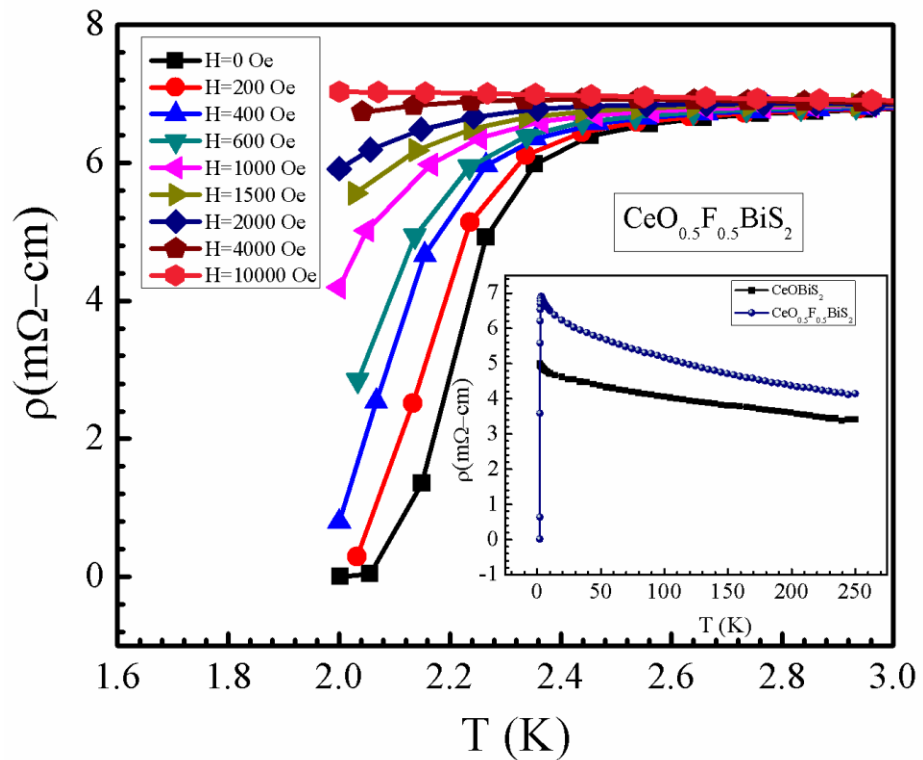


Figure 3(b):

